Sensors and Actuators A 165 (2011) 310–315

Contents lists available at ScienceDirect

Sensors and Actuators A: Physical

journal homepage: www.elsevier.com/locate/sna

Short communication

Electroosmotic pump performance is affected by concentration polarizations of both electrodes and pump

Matthew E. Suss, Ali Mani, Thomas A. Zangle[1], Juan G. Santiago*

Dept. of Mechanical Engineering, Stanford University, Stanford, CA 94305-3030, USA

ARTICLE INFO

Article history:
Received 12 June 2010
Received in revised form
28 September 2010
Accepted 6 October 2010
Available online 14 October 2010

Keywords:
Electroosmotic pump
Electrokinetic pump
Concentration polarization
Electrodes
Electrode concentration polarization
Dukhin number
Electrolysis

ABSTRACT

Current methods of optimizing electroosmotic (EO) pump performance include reducing pore diameter and reducing ionic strength of the pumped electrolyte. However, these approaches each increase the fraction of total ionic current carried by diffuse electric double layer (EDL) counterions. When this fraction becomes significant, concentration polarization (CP) effects become important, and traditional EO pump models are no longer valid. We here report on the first simultaneous concentration field measurements, pH visualizations, flow rate, and voltage measurements on such systems. Together, these measurements elucidate key parameters affecting EO pump performance in the CP dominated regime. Concentration field visualizations show propagating CP enrichment and depletion fronts sourced by our pump substrate and traveling at order mm/min velocities through millimeter-scale channels connected serially to our pump. The observed propagation in millimeter-scale channels is not explained by current propagating CP models. Additionally, visualizations show that CP fronts are sourced by and propagate from the electrodes of our system, and then interact with the EO pump-generated CP zones. With pH visualizations, we directly detect that electrolyte properties vary sharply across the anode enrichment front interface. Our observations lead us to hypothesize possible mechanisms for the propagation of both pump- and electrode-sourced CP zones. Lastly, our experiments show the dynamics associated with the interaction of electrode and membrane CP fronts, and we describe the effect of these phenomena on EO pump flow rates and applied voltages under galvanostatic conditions.

1. Introduction

Electroosmotic (EO) micropumps require no moving parts, can be fabricated cheaply and compactly, and can deliver relatively high flow rates and pressures [1,2]. EO pumps can also be used in applications requiring fairly low applied voltage (a few volts) and low applied power per volume flow rate [3]. A disadvantage of EO pumps, particularly in applications requiring high pump current density, is that electrolysis bubbles may eventually grow at a rate which interferes with pump performance [4,5], and that long-term pumping can create electrochemically sourced pH gradients in the system [6]. EO pump systems often consist of a porous oxide structure, or frit, between two electrodes. The applied field exerts a Coulombic force on mobile counterions of electric double layers (EDL), and ion drag creates bulk fluid flow.

Recent work on EO pump optimizations have concluded that higher flow rate per power can often be achieved by: (i) reducing frit pore size, and (ii) reducing the ionic strength of the pumped electrolyte [7–9]. For example, Litster et al. [3], using a silica EO pump with 450 nm mean pore diameter and 1 mM ionic strength electrolyte, demonstrated the delivery of 10 μl/min and a few kPa pressure capacity with applied potential and power of 3 V and 75 μW, respectively. Each of the optimization strategies above increases the fraction of total ionic current carried by excess counterions shielding the wall charge, and thus increases the ratio of conductivity due to surface counterions to the conductivity due to bulk ions. This ratio for a binary electrolyte in a porous frit can be expressed as [11,12]:

$$Du = \frac{z_1 \upsilon_1 \left(|s|/l\right)}{Fc_o(z_1^2 \upsilon_1 + z_2^2 \upsilon_2)} \quad (1)$$

Which is related to Dukhin number (but only equal in the limit of high zeta [10]). To express this ratio in a simple manner, we assumed a spatially uniform surface charge density, s. The parameter l is a length scale representing the ratio of total electrolyte volume in the porous media to pore surface area [12], c_o is the pore centerline electrolyte concentration (for non-overlapped

* Corresponding author at: 440 Escondido Mall, Bldg 530, rm 224, Stanford, CA 94305, USA. Tel.: +1 650 723 5689; fax: +1 650 723 7657.
E-mail address: juan.santiago@stanford.edu (J.G. Santiago).
[1] Present address: Department of Pathology & Laboratory Medicine, University of, California, Los Angeles, CA 90095, USA.

0924-4247/$ – see front matter © 2010 Elsevier B.V. All rights reserved.
doi:10.1016/j.sna.2010.10.002

EDLs), υ is ionic mobility, z is ionic charge, and F is Faraday's constant. Subscript 1 denotes the counter-ion and 2 the co-ion. Therefore, optimizing EO pumps by decreasing pore size (decreasing l), or decreasing electrolyte ionic strength (c_o), increases the ratio described by Eq. (1). If this ratio becomes order unity or higher, concentration polarization (CP) effects become significant [11,13]. In this regime, traditional models for EO pumps [8,9], which ignore this phenomenon, no longer hold.

Applying an electric field to a frit with significant surface conductivity results in a higher flux of counterions than coions through the frit. For a negatively charged frit surface (typical of porous glass), this flux imbalance causes the formation of depletion and enrichment zones, respectively at the anode and cathode sides of the frit [12,14]. This effect is known as electrokinetic or ion concentration polarization (CP) [15,16]. Mani et al. [11] and Zangle et al. [13] investigated CP in serial micro-nano-microchannel systems. They confirmed that, at nanochannel Dukhin numbers of roughly unity and above, CP can propagate in the form of shocks, featuring long-range growth of enrichment and depletion zones emanating from the nanochannel. However, few studies have focused on the effect of CP on EO pumps. Postler et al. [17] performed a numerical study of EO flow in a submicron channel, which showed non-linearity in EOF velocity with applied field. They attributed this non-linearity to surpassing the limiting current of the submicron channel. Strickland et al. [12] presented brief qualitative fluorescence visualizations which showed the formation of propagating CP fronts from a porous glass EO pump with roughly 500 nm diameter pores, while pumping 0.1 to 1 mM sodium borate buffer. Additionally, Litster et al. [3] observed distinct transients in EO pump flow rate when using a frit with submicron sized pores, which they hypothesized could be due to CP effects.

In this paper, we provide new quantitative experimental characterization of CP in EO pumps under galvanostatic conditions using simultaneous visualizations, flow rate and voltage measurements. We observe, at sufficiently high Du, a long-range propagation of enrichment and depletion fronts starting from the membrane through the connecting millimeter-scale channel (hereafter "millichannel"). Recently, Mani et al. [11] developed a theory explaining one mechanism for propagation of CP in systems involving micro and nano-scale channels. However, as we shall see, for our system their model is not applicable as our millichannel has negligible EDL current transport. Further, we show that fronts of perturbed concentration and pH are sourced by, and propagate from, the electrodes of our system. We show direct evidence of a sharp jump in electrolyte chemistry, in addition to a jump in electrolyte ionic strength, across the propagating anode enrichment front. We speculate as how this latter observation may explain the mechanism of millichannel CP propagation. Lastly, we report what is to our knowledge the first CP visualization combined with flow rate and voltage measurements. With these measurements, we elucidate key parameters affecting pump performance in the CP regime and show a scaling which collapses performance transients across all our experimental conditions.

2. Experimental setup

Fig. 1 is a schematic of our experimental setup. We used a porous silica frit with mean pore radius of 225 nm (EoPlex, Redwood City, CA), similar to that used in studies by Litster et al. [3] and Strickland et al. [12]. The 1 mm thick frits were epoxied with clear UV cure epoxy (Norland, Cranbury NJ) into a clear, 5 mm × 5 mm square, borosilicate glass millichannel (Freidrich and Dimmock, Millville NJ). The frits were saturated with deionized (DI) water (Fischer Scientific, Waltham, MA) prior to the epoxy step to minimize the degree to which epoxy invaded the pores. Electrodes were made of coiled platinum, with coils approximately a millimeter apart,

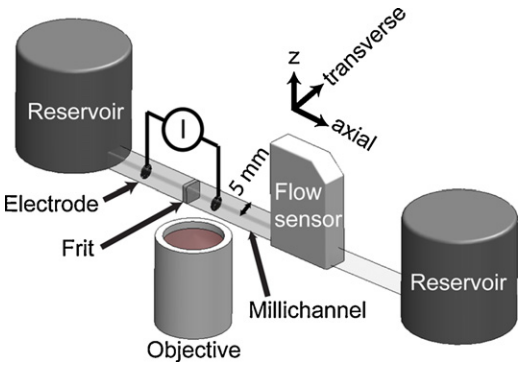

Fig. 1. Schematic of the experimental setup used to perform simultaneous visualizations of concentration and qualitative pH fields, flow rate measurements, and voltage measurements under galvanostatic conditions. The frit was epoxied into a 5 mm square, clear borosilicate glass channel, and coiled platinum wire electrodes were positioned at variable locations along the channel. Visualizations were performed with an inverted epifluorescence microscope, and flow rate measurements were performed with a microflow sensor. Large diameter reservoirs were filled to equal heights to insure a negligible external pressure load.

and inserted into the millichannel at various distances from the frit surface (cf. legend of Fig. 4). Two large diameter (3 cm) cylindrical end-channel reservoirs were filled to equal heights to insure no significant external pressure was applied to the pump system during operation. During experiments, we used 0.1–10 mM (Na^+ concentration) sodium tetraborate decahydrate buffer (Mallinckrodt, Hazelwood, MO) to set ionic strength, where the borate salt was diluted in DI water. Our DI water had an initial, typical pH of 5.3 [18]. Our electrolyte solutions had pH values ranging from 5.5 to 9.2 for, respectively, 0.1 mM and 10 mM tetraborate decahydrate. We pumped with constant currents from 25 to 100 μA and measured applied potential with a Keithley 2410 sourcemeter (Cleveland, OH). Before each realization, we used a syringe pump (Harvard Apparatus, Holliston, MA) to flow at least 0.5 ml of new electrolyte through the frit. When switching to a borate solution of different ionic strength, we used first pressure-driven flow and then electroosmotic flow to each drive at least 0.5 mL of new solution through the frit. We found that the above pre-treatment allowed for repeatable flow rate versus time measurements, both in flow rate magnitude and transients observed (as will be shown in Section 3.3). A micro flow sensor (ASL 1430-16, Sensirion, Switzerland) was used downstream of the pump to measure flow rate at a sampling frequency of 1 Hz.

Simultaneous to our flow rate and voltage measurements, we obtained images of concentration and qualitative pH fields about our frit. We did not obtain concentration and pH field data within our frit, as the porous silica was effectively opaque. For all visualizations, we used an inverted epifluorescent microscope (Eclipse TE300, Nikon, Japan), a 1×, NA 0.04 objective (Nikon, Japan), and captured images with a CCD camera (MicroMAX, Princeton Instruments, Trenton, NJ) with a 6.7 μm pixel size. For simple concentration field visualizations (Fig. 2), we used an XF23 filter cube (Omega Optical, Brattleboro, VT) with peak excitation and emission wavelength ranges of 475–500 and 515–550 nm, respectively. Also, for simple concentration field visualizations (Fig. 2), we observed the anionic, pH insensitive [19] tracing dye Alexa Fluor 488 (Invitrogen, Carlsbad, CA). The dye was at a concentration of 4 μM, over an order of magnitude lower than that of the sodium borate. For simultaneous pH and concentration field visualizations (Fig. 3), we used instead an XF53 dual pass filter cube (Omega Optical) with peak excitation wavelength ranges of 475–500 and 550–600 nm, and peak emission wavelength ranges of 500–550 and 600–675 nm, and a quad view (Micro-Imager, Photometrics, Tucson, AZ) to spatially separate concentration and pH field signals onto separate quad-